



Title	In situ x-ray photoelectron spectroscopy for electrochemical reactions in ordinary solvents
Author(s)	Masuda, Takuya; Yoshikawa, Hideki; Noguchi, Hidenori; Kawasaki, Tadahiro; Kobata, Masaaki; Kobayashi, Keisuke; Uosaki, Kohei
Citation	Applied Physics Letters, 103(11), 111605 https://doi.org/10.1063/1.4821180
Issue Date	2013-09-09
Doc URL	http://hdl.handle.net/2115/59735
Rights	Copyright 2013 American Institute of Physics. This article may be downloaded for personal use only. Any other use requires prior permission of the author and the American Institute of Physics. The following article appeared in Appl. Phys. Lett. 103, 111605, 2013, and may be found at http://dx.doi.org/10.1063/1.4821180
Type	article
File Information	APL_103_11605.pdf



[Instructions for use](#)

In situ x-ray photoelectron spectroscopy for electrochemical reactions in ordinary solvents

Takuya Masuda, Hideki Yoshikawa, Hidenori Noguchi, Tadahiro Kawasaki, Masaaki Kobata, Keisuke Kobayashi, and Kohei Uosaki

Citation: *Applied Physics Letters* **103**, 111605 (2013); doi: 10.1063/1.4821180

View online: <http://dx.doi.org/10.1063/1.4821180>

View Table of Contents: <http://scitation.aip.org/content/aip/journal/apl/103/11?ver=pdfcov>

Published by the AIP Publishing

Articles you may be interested in

Hard x-ray photoelectron spectroscopy using an environmental cell with silicon nitride membrane windows
J. Appl. Phys. **117**, 234902 (2015); 10.1063/1.4922335

An ultra-high vacuum electrochemical flow cell for in situ/operando soft X-ray spectroscopy study
Rev. Sci. Instrum. **85**, 043106 (2014); 10.1063/1.4870795

Optical properties of silicon nanocrystals in silica: Results from spectral filtering effect, m-line technique, and x-ray photoelectron spectroscopy
J. Appl. Phys. **104**, 104316 (2008); 10.1063/1.3010304

X-ray photoelectron spectroscopy study of dielectric constant for Si compounds
Appl. Phys. Lett. **89**, 154103 (2006); 10.1063/1.2361177

X-ray photoelectron spectroscopy study of rapid thermal annealed silicon–silicon oxide systems
J. Appl. Phys. **81**, 7386 (1997); 10.1063/1.365278



In situ x-ray photoelectron spectroscopy for electrochemical reactions in ordinary solvents

Takuya Masuda,^{1,2} Hideki Yoshikawa,³ Hidenori Noguchi,^{1,2,4,5} Tadahiro Kawasaki,⁶ Masaaki Kobata,³ Keisuke Kobayashi,³ and Kohei Uosaki^{1,4,5,a)}

¹Global Research Center for Environment and Energy Based on Nanomaterials Science (GREEN), National Institute for Materials Science (NIMS), Tsukuba 305-0044, Japan

²PRESTO, Japan Science and Technology Agency (JST), 4-1-8 Honcho, Kawaguchi, Saitama 333-0012, Japan

³Synchrotron X-ray Station at SPring-8, National Institute for Materials Science (NIMS), Sayo, Hyogo 679-5148, Japan

⁴Graduate School of Chemical Sciences and Engineering, Hokkaido University, Sapporo, Hokkaido 060-0810, Japan

⁵International Center for Materials Nanoarchitectonics (WPI-MANA), National Institute for Materials Science (NIMS), Tsukuba, Ibaraki 305-0044, Japan

⁶Graduate School of Engineering, Nagoya University, Furo-cho, Chikusa, Nagoya 464-8603, Japan

(Received 10 March 2013; accepted 25 August 2013; published online 12 September 2013)

In situ electrochemical X-ray photoelectron spectroscopy (XPS) apparatus, which allows XPS at solid/liquid interfaces under potential control, was constructed utilizing a microcell with an ultra-thin Si membrane, which separates vacuum and a solution. Hard X-rays from a synchrotron source penetrate into the Si membrane surface exposed to the solution. Electrons emitted at the Si/solution interface can pass through the membrane and be analyzed by an analyzer placed in vacuum. Its operation was demonstrated for potential-induced Si oxide growth in water. Effect of potential and time on the thickness of Si and Si oxide layers was quantitatively determined at sub-nanometer resolution. © 2013 AIP Publishing LLC. [<http://dx.doi.org/10.1063/1.4821180>]

Many important processes such as electrochemical energy conversion, corrosion, and biological processes take place at solid-liquid interfaces.¹ Understanding of these processes at the atomic level is not only scientifically important but is also the key to improving the performance of next generation energy conversion devices such as fuel cells, Li-air batteries, dye-sensitized solar cells, and photocatalysts. Information on the geometric, electronic, and molecular structures at a solid/liquid interface are essential to clarify these processes.¹

X-ray photoelectron spectroscopy (XPS) is the most powerful technique for the determination of surface compositions, oxidation states, and electronic structures of materials of interest with very high surface sensitivity.² Since the 1970s, “electrochemical photoelectron spectroscopy” has been developed³ and utilized not only for fundamental interest⁴ but also for practical applications such as electrocatalysts for fuel cells.⁵ Usually, samples can be transferred from an electrochemical chamber in an ambient atmosphere to an analysis chamber kept in vacuum immediately after the electrochemical treatments without being exposed to air so that any contamination of the surface from exposure to open air can be avoided. However, structure and oxidation state of the electrode surface may be changed during the transfer from the solution, where the electrode is under electrochemically controlled conditions, to vacuum, where potential control is not possible. Ambient pressure (AP)-XPS, which allows measurements at a solid-gas interface including adsorbed water molecules on solid surfaces⁶ and at a liquid-gas interface,⁷ has been also developed since the 1970s⁸ by

utilizing a differential pumping system.⁹ Although AP-XPS has been used to study electrochemical processes at solid/vapor interfaces,¹⁰ those at solid/liquid interfaces cannot be observed by this method because it is difficult to control the thickness of water on solid electrode surfaces in vacuum. *In situ* electrochemical XPS has been performed using room temperature ionic liquids (RTILs) as the electrolyte solution¹¹ because of their non-volatility (near zero vapor pressure) and high ionic conductivity.¹² Although these results are important, this methods cannot be generalized as most of the important electrochemical processes take place in ordinary solutions of both aqueous and non-aqueous solvents in which the physical and chemical properties of materials are significantly different from those in RTILs.

Here, we report a “real” *in situ* electrochemical XPS apparatus for the measurements at solid/liquid interface under electrochemical condition using hard X-rays¹³ and a micro-volume cell equipped with an ultrathin Si membrane.

The conceptual design of the present *in situ* electrochemical XPS arrangement is illustrated in Figure 1(A). A micro-volume cell filled with a liquid is sealed by a 15-nm-thick Si membrane, which serves as a separator between vacuum and ambient, a window for X-rays and photoelectrons, and a working electrode. The cell is placed in a vacuum XPS apparatus, and synchrotron radiation (SR) hard X-ray is irradiated to the vacuum side of the membrane. X-rays penetrate to the solution side through the membrane, and photoelectrons emitted from Si exposed to the solution, i.e., at solid/liquid interface, can pass through the Si membrane, if the thickness of the membrane is thin enough, and can then be collected and analyzed by a hemispherical photoelectron analyzer (VG Scienta R4000). The total photoelectron signal will also contain those generated inside and at the vacuum side of the membrane.

a) Author to whom correspondence should be addressed. Electronic mail: uosaki.kohei@nims.go.jp. Tel.: +81-29-860-4301. Fax: +81-29-851-3362.

Figure 1(B) shows the inelastic mean free paths (IMFPs) calculated from optical data for Si, SiO₂, and Si₃N₄.¹⁴ In conventional XPS, since Mg and Al with photon energies of 1.25 and 1.49 keV, respectively, are generally used as X-ray targets, the kinetic energies of photoelectrons are <1 keV and, therefore, the IMFPs are ca. 1 nm, which is too short to pass through the 15-nm-thick Si membrane. On the other hand, if hard X-rays from a synchrotron source with a photon energy of ~6 keV are used, much longer IMFPs are expected. For example, the IMFP of photoelectron with a kinetic energy of 4.1 keV is 7.5 nm, and 14% of photoelectrons emitted at the solution side of the Si can reach the vacuum side in the present experiment where the 15 nm-thick Si membrane was used.

The energy resolution was 245 meV, as experimentally determined by measuring the spectra of the Au valence band at the Fermi level. The X-ray incidence angle, as measured from the sample surface, was fixed at 4°. All the measurements were carried out at an incident X-ray energy of 5950.1 eV at the BL15XU beamline at SPring-8.¹⁵ The high photon flux of ~10¹¹ photons/s is another advantage of using SR.

Figures 1(C) and 1(D) show top and side views of the Si membrane (SiMPore) and the micro-volume *in situ* XPS cell, respectively, used in the present study. After the surface of the Si membrane was made hydrophilic by plasma ion treatment (PIB-10, Vacuum Device), a droplet of water purified using a Milli-Q system (Yamato, WRX-10) was placed on the membrane and sealed by conductive Cu tape (Seiwa Electric MFG).¹⁶ The presence of water was confirmed by optical microscopy which showed that the Si membrane was stretched by the presence of water. Indium gallium eutectic alloy was pasted on the frame of the Si membrane, and electrical contact to the potentiostat was achieved by bonding a Au wire. A bias voltage application was performed as previously reported.¹⁷ The potential of the Si membrane with respect to the Cu tape was controlled by a potentiostat (HSV-110, Hokuto Denko).

Figure 2(A) shows a current-potential (I-V) relation of the Si membrane in contact with water (blue). Anodic current started to increase from about 0.8 V. Since the I-V curve was measured in a two electrode system, the electrode potential of each electrode, Si membrane, and Cu tape cannot be determined. However, it is expected that Si oxide formation and hydrogen evolution reaction took place at the Si membrane and Cu tape, respectively, when anodic current flowed at the Si membrane.¹⁸ I-V relation of the micro-volume cell without water (red) was also measured, and no current was observed even when the positive potential limit was extended, showing that the Si and Cu film were insulated from each other by adhesive of Cu tape.

Figure 2(B) shows photoelectron spectra in the Si 2p region of the Si membrane measured at various potentials.¹⁹ Doublet peaks corresponding to Si 2p_{3/2} and 2p_{1/2} were observed at 100 and 99.5 eV, respectively. Even before the potential was applied, a broad peak due to native oxide was observed around 104.5 eV. This peak increased as the potential became more positive (Figure 2(C)), showing the growth of Si oxide by electrochemical oxidation at the Si membrane/water interface. SR-induced etching of semiconductor surfaces²⁰ and reduction of Si oxide²¹ were previously reported. If similar processes took place in the present study, the peak around 104.5 eV should decrease but actually increased, confirming the electrochemical growth of Si oxide. Moreover, SR was off after the measurement of spectrum (g) of Figure 2(B) until that of spectrum (h) with keeping the potential at 1500 mV, and the largest growth of Si oxide was observed in this period. Thus, it is reasonable to consider that the Si oxide was electrochemically grown, and above-mentioned processes have only subtle effect.

In addition, although the ratio of Si 2p_{3/2} and 2p_{1/2} should be constant, the peak at 100 eV slightly increased (inset of Figure 2(B)), implying the appearance of additional components which overlap with the Si 2p_{3/2}. Figure 2(D) shows difference spectra under various conditions used to remove the contribution of SR of the native oxide and to highlight

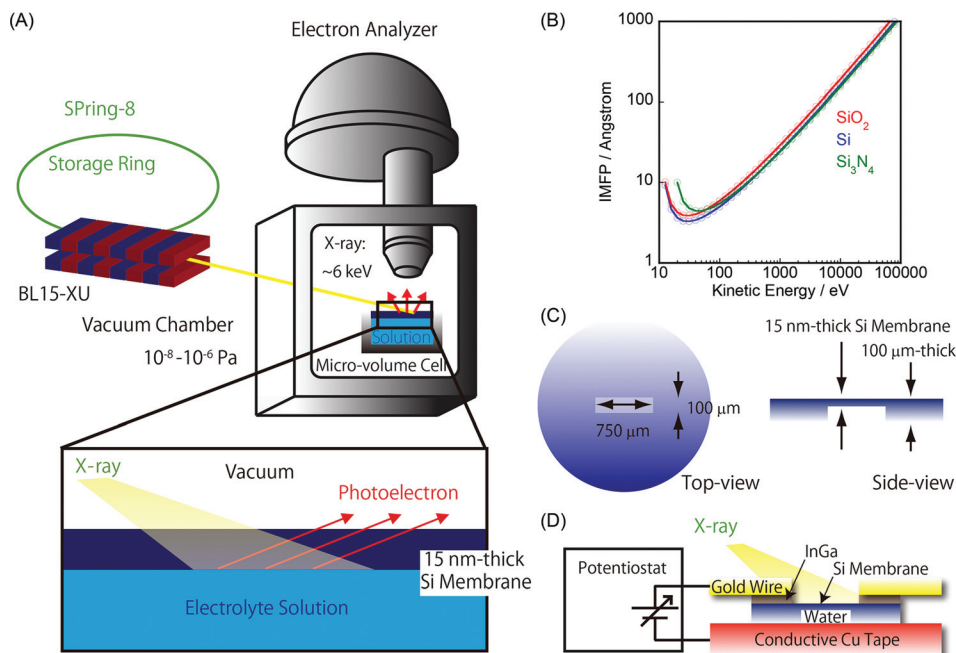


FIG. 1. Schematic illustration of (A) *in situ* XPS apparatus. (B) IMFPs calculated from optical data for Si, SiO₂, and Si₃N₄. (C) Si membrane and (D) micro-volume *in situ* XPS cell.

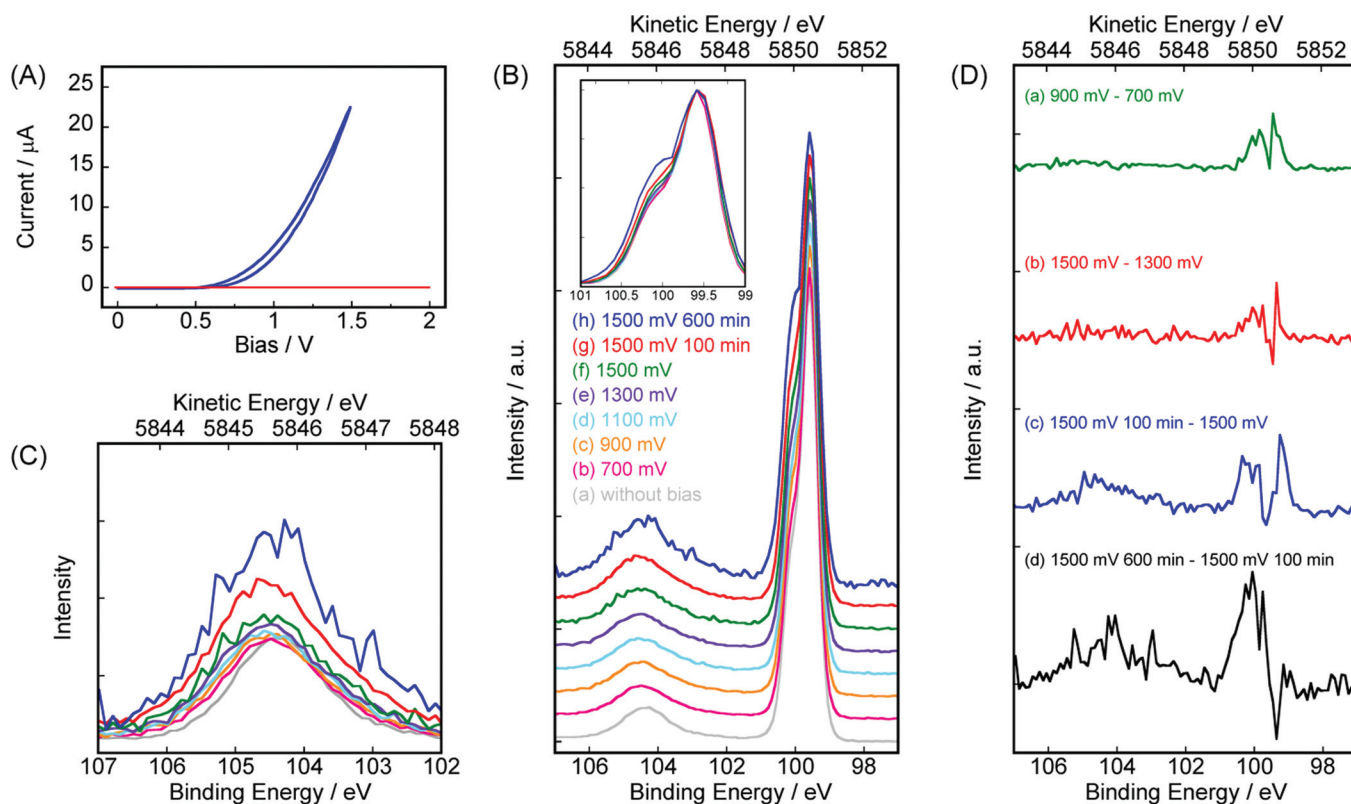


FIG. 2. (A) I-V relationships of the micro-volume cell with (blue) and without water (red), measured in the configuration of Figure 1(D). (B) Photoelectron spectra in the Si $2p_{3/2}$ region of the Si membrane measured (a) without bias and at (b) 700 mV, (c) 900 mV, (d) 1100 mV, (e) 1300 mV, and (f) 1500 mV and after keeping the potential at 1500 mV for (g) 100 min and (h) 600 min. Inset: Magnified image of (B) in the region between 101 and 99 eV. (C) Magnified image of (B) in the region between 107 and 102 eV, corresponding to Si^{4+} . (D) Difference spectra at various conditions.

the change in spectral shape by electrochemical oxidation of the Si membrane. In the difference between the spectra taken at 900 mV and 700 mV, additional components were found around 100 and 99.3 eV. These peaks are considered to be due to strained interfacial Si atoms, as previously proposed.²² When the potential was made to be 1500 mV from 1300 mV, the peak at 104.5 eV increased with time, confirming the growth of Si oxide.

Figure 3 shows schematic models of the Si membrane in a cross-sectional view. Before the oxidation (Fig. 3(A)),

a cross-section of the 15-nm-thick Si membrane can be illustrated as a three layer model based on the assumption that both the vacuum and solution sides are covered by native oxide layers with a thickness of d nm. When the Si membrane is positively biased (Fig. 3(B)), the thickness of layer B, i.e., Si, decreased by a nm and that of layer C, i.e., Si oxide, increased by $2.2a$ nm due to the difference between the Si densities of Si and Si oxide.²³ The photoelectron intensity ratio, $I_{\text{SiO}_2}/I_{\text{Si}}$, is represented by Eq. (1)¹⁶

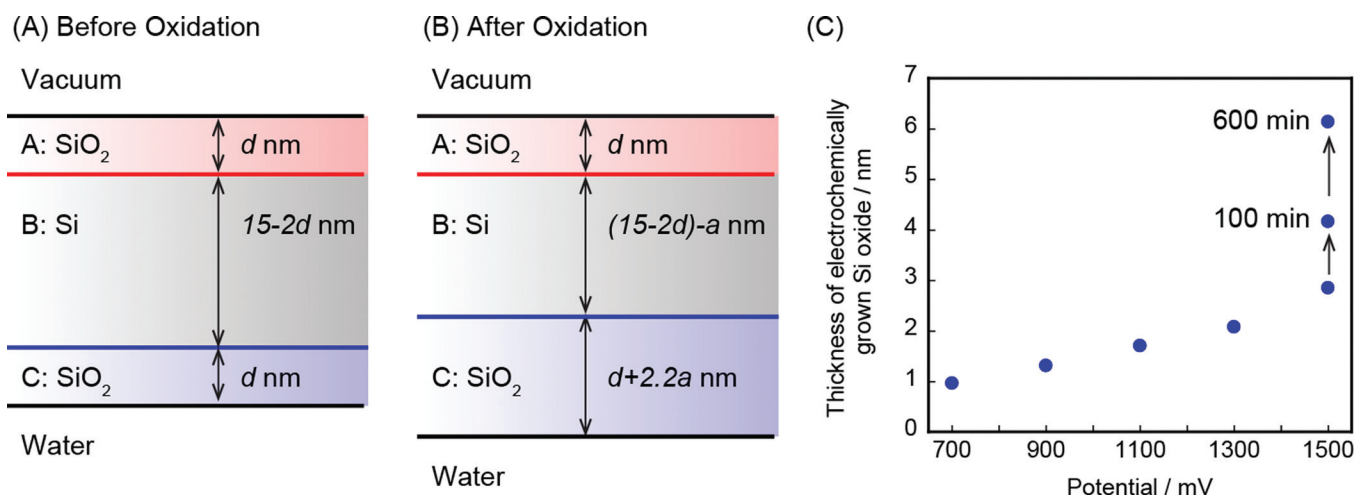


FIG. 3. Schematic models of the Si membrane (A) before and (B) after the oxidation. (C) Thickness of electrochemically grown Si oxide calculated from Eq. (1).

$$\frac{I_{SiO_2}}{I_{Si}} = \frac{N_{SiO_2} \times \lambda_{SiO_2} [1 - \exp(-d/\lambda_{SiO_2})] + N_{SiO_2} \times \lambda_{SiO_2} [1 - \exp(-(d+2.2a)/\lambda_{SiO_2})] \times \exp(-d/\lambda_{SiO_2}) \times \exp(-(15-2d-a)/\lambda_{Si})}{N_{Si} \times \lambda_{Si} [1 - \exp(-(15-2d-a)/\lambda_{Si})] \times \exp(-d/\lambda_{SiO_2})}, \quad (1)$$

where λ_{SiO_2} (12.2 nm) and λ_{Si} (10.3 nm) are the inelastic mean free paths of the Si 2p photoelectrons for Si oxide and Si, obtained using the TPP-2M formula,²⁴ and N_{SiO_2} (2.28×10^{22} atoms/cm³) and N_{Si} (5.00×10^{22} atoms/cm³) are the Si densities in Si oxide and Si,²³ respectively. The photoelectron intensities of the Si oxide from the layers A and C, I_{SiO_2} , and of Si from layer B, I_{Si} , are obtained by integrating the Si⁴⁺ peak and the doublet peaks corresponding to the Si 2p_{3/2} and 2p_{1/2}, respectively. Thus, the thickness of electrochemically grown Si oxide can be quantitatively determined, as shown in Figure 3(C). The potential and time-dependent thickness of each layer, reflecting the anodic growth of the oxide, was summarized in Figure S2 of supplementary material.¹⁶

In conclusion, we have constructed an XPS system for *in situ* measurements at a solid-liquid interface under controlled electrochemical conditions. We have also presented the report of the use of *in situ* electrochemical XPS by performing a quantitative analysis of the electrochemical growth of Si oxide in real time as a demonstration of this system's capabilities. At present, the cell-volume is minimized to prevent any damage possibly being caused by unexpected breakage of the membrane due to the pressure gap between the inside and outside of the cell. A flow-type cell which enables injection of additional reactants from outside of the vacuum apparatus is currently under development as well as the provision of a safety device in case of breakage.

The present work was partially supported by World Premier International Research Center (WPI) Initiative on Materials Nanoarchitectonics and MEXT Program for Development of Environmental Technology using Nanotechnology from Ministry of Education, Culture, Sports, Science and Technology, Japan. Synchrotron radiation experiments were performed as projects approved by the Japan Synchrotron Radiation Research Institute (JASRI) (Proposal Nos. 2011A4608 and 2011B4609).

¹H. D. Abruna, *Electrochemical Interfaces: Modern Techniques for In Situ Interface Characterization* (VCH Publishers, New York/Weinheim/Cambridge, 1991).

²S. Hüfner, *Photoelectron Spectroscopy, Principles and Applications*, 3rd ed. (Springer-Verlag, Berlin/Heidelberg/New York, 2003).

³R. M. Ishikawa and A. T. Hubbard, *J. Electroanal. Chem.* **69**(3), 317 (1976).

⁴A. Wieckowski, *Interfacial Electrochemistry: Experimental, Theory and Applications* (Marcel Dekker, New York, 1999).

⁵M. Wakisaka, Y. Udagawa, H. Suzuki, H. Uchida, and M. Watanabe, *Energy Environ. Sci.* **4**(5), 1662 (2011).

⁶G. Ketteler, D. F. Ogletree, H. Bluhm, H. J. Liu, E. L. D. Hebenstreit, and M. Salmeron, *J. Am. Chem. Soc.* **127**(51), 18269 (2005); G. Ketteler, S. Yamamoto, H. Bluhm, K. Andersson, D. E. Starr, D. F. Ogletree, H. Ogasawara, A. Nilsson, and M. Salmeron, *J. Phys. Chem. C* **111**(23), 8278

(2007); S. Yamamoto, K. Andersson, H. Bluhm, G. Ketteler, D. E. Starr, T. Schiros, H. Ogasawara, L. G. M. Pettersson, M. Salmeron, and A. Nilsson, *ibid.* **111**(22), 7848 (2007); *J. Phys.: Condens. Matter* **20**(18), 184025 (2008); S. Porsgaard, P. Jiang, F. Borondics, S. Wendt, Z. Liu, H. Bluhm, F. Besenbacher, and M. Salmeron, *Angew. Chem., Int. Ed.* **50**(10), 2266 (2011); T. Shimada, B. S. Mun, I. F. Nakai, A. Banno, H. Abe, Y. Iwasawa, T. Ohta, and H. Kondoh, *J. Phys. Chem. C* **114**(40), 17030 (2010); R. Toyoshima, M. Yoshida, Y. Monya, Y. Kousa, K. Suzuki, H. Abe, B. S. Mun, K. Mase, K. Amemiya, and H. Kondoh, *ibid.* **116**(35), 18691 (2012).

⁷M. J. Krisch, R. D'Auria, M. A. Brown, D. J. Tobias, J. C. Hemminger, M. Ammann, D. E. Starr, and H. Bluhm, *J. Phys. Chem. C* **111**(36), 13497 (2007); S. Ghosal, M. A. Brown, H. Bluhm, M. J. Krisch, M. Salmeron, P. Jungwirth, and J. C. Hemminger, *J. Phys. Chem. A* **112**(48), 12378 (2008).

⁸H. Siegbahn and K. Siegbahn, *J. Electron Spectrosc. Relat. Phenom.* **2**(3), 319 (1973); H. Siegbahn, L. Asplund, P. Kelfve, K. Hamrin, L. Karlsson, and K. Siegbahn, *ibid.* **5**, 1059 (1974); H. Siegbahn, L. Asplund, P. Kelfve, and K. Siegbahn, *ibid.* **7**(5), 411 (1975).

⁹D. F. Ogletree, H. Bluhm, G. Lebedev, C. S. Fadley, Z. Hussain, and M. Salmeron, *Rev. Sci. Instrum.* **73**(11), 3872 (2002); M. Salmeron and R. Schlogl, *Surf. Sci. Rep.* **63**(4), 169 (2008).

¹⁰C. J. Zhang, M. E. Grass, A. H. McDaniel, S. C. DeCaluwe, F. El Gabaly, Z. Liu, K. F. McCarty, R. L. Farrow, M. A. Linne, Z. Hussain, G. S. Jackson, H. Bluhm, and B. W. Eichhorn, *Nature Mater.* **9**(11), 944 (2010); Y. C. Lu, E. J. Crumlin, G. M. Veith, J. R. Harding, E. Mutoro, L. Baggetto, N. J. Dudney, Z. Liu, and Y. Shao-Horn, *Sci. Rep.* **2**, 715 (2012).

¹¹A. W. Taylor, F. L. Qiu, I. J. Villar-Garcia, and P. Licence, *Chem. Commun.* **45**(39), 5817 (2009); D. Weingarh, A. Foelske-Schmitz, A. Wokaun, and R. Kotz, *Electrochem. Commun.* **13**(6), 619 (2011); R. Wibowo, L. Aldous, R. M. J. Jacobs, N. S. A. Manan, and R. G. Compton, *Chem. Phys. Lett.* **517**(1–3), 103 (2011).

¹²K. R. J. Lovelock, I. J. Villar-Garcia, F. Maier, H. P. Steinruck, and P. Licence, *Chem. Rev.* **110**(9), 5158 (2010); S. Kuwabata, T. Tsuda, and T. Torimoto, *J. Phys. Chem. Lett.* **1**(21), 3177 (2010).

¹³K. Kobayashi, M. Yabashi, Y. Takata, T. Tokushima, S. Shin, K. Tamasaku, D. Miwa, T. Ishikawa, H. Nohira, T. Hattori, Y. Sugita, O. Nakatsuka, A. Sakai, and S. Zaima, *Appl. Phys. Lett.* **83**(5), 1005 (2003); K. Kobayashi, *Nucl. Instrum. Methods Phys. Res. A* **547**(1), 98 (2005).

¹⁴D. Briggs and J. T. Grant, *Surface Analysis by Auger and X-Ray Photoelectron Spectroscopy* (IM Publications, Chichester, 2003).

¹⁵A. X. Gray, C. Papp, S. Ueda, B. Balke, Y. Yamashita, L. Plucinski, J. Minar, J. Braun, E. R. Ylvisaker, C. M. Schneider, W. E. Pickett, H. Ebert, K. Kobayashi, and C. S. Fadley, *Nature Mater.* **10**(10), 759 (2011).

¹⁶See supplementary material at <http://dx.doi.org/10.1063/1.4821180> for details of the micro-volume cell filled with water and derivation of Eq. (1).

¹⁷T. Nagata, M. Haemori, Y. Yamashita, H. Yoshikawa, Y. Iwashita, K. Kobayashi, and T. Chikyow, *Appl. Phys. Lett.* **97**(8), 082902 (2010); **99**(22), 223517 (2011); *J. Appl. Phys.* **113**(16), 163707 (2013).

¹⁸Since not only the 15 nm-thick Si membrane but also the frame is in contact with water, the I-V data are representative of the membrane and frame.

¹⁹All the spectra were normalized at the Si 2p_{1/2} peak.

²⁰Q. Ma, N. Moldovan, D. C. Mancini, and R. A. Rosenberg, *J. Appl. Phys.* **89**(5), 3033 (2001).

²¹Y. Sugita, Y. Nara, N. Nakayama, and T. Ito, *Jpn. J. Appl. Phys. Part 1* **30**(11B), 3209 (1991).

²²J. H. Oh, H. W. Yeom, Y. Hagimoto, K. Ono, M. Oshima, N. Hirashita, M. Nywa, A. Toriumi, and A. Kakizaki, *Phys. Rev. B* **63**(20), 205310 (2001).

²³F. J. Himpsel, F. R. Mcfeely, A. Talebibrabimi, J. A. Yarmoff, and G. Hollinger, *Phys. Rev. B* **38**(9), 6084 (1988).

²⁴S. Tanuma, C. J. Powell, and D. R. Penn, *Surf. Interface Anal.* **11**(11), 577 (1988); C. J. Powell and A. Jablonski, *Nucl. Instrum. Methods Phys. Res. A* **601**(1–2), 54 (2009).